Observation of a threshold enhancement in the $p\overline{p}$ mass spectrum from $J/\psi \to \gamma p\overline{p}$

J. Z. Bai[1], Y. Ban[11], J. G. Bian[1], A. D. Chen[1], H. F. Chen[17], H. S. Chen[1], J. Chen[5], J. C. Chen[1], X. D. Chen[1], Y. B. Chen[1], B. S. Cheng[1], S. P. Chi[1], Y. P. Chu[1], J. B. Choi[4], X. Z. Cui[1], Y. S. Dai[20], L. Y. Dong[1], Z. Z. Du[1], W. Dunwoodie[15], H. Y. Fu[1], L. P. Fu[8], C. S. Gao[1], S. D. Gu[1], Y. N. Guo[1], Z. J. Guo[1], S. W. Han[1], Y. Han[1], F. A. Harris[16], J. He[1], J. T. He[1], K. L. He[1], M. He[11], X. He[1], T. Hong[1], Y. K. Heng[1], G. Y. Hu[1], H. M. Hu[1], Q. H. Hu[1], T. Hu[1], G. S. Huang[3], X. P. Huang[1], Y. Z. Huang[1], J. M. Izen[18], X. B. Ji[13], C. H. Jiang[1], Y. Jin[1], B. D. Jones[18], J. S. Kang[9], Z. J. Ke[1], H. J. Kim[14], S. K. Kim[14], T. Y. Kim[14], Y. F. Lai[1], D. Li[1], H. B. Li[1], H. H. Li[7], J. Li[1], J. C. Li[1], P. Q. Li[1], Q. J. Li[1], R. Y. Li[1], W. Li[1], W. G. Li[1], X. N. Li[1], X. Q. Li[10], B. Liu[1], F. Liu[7], Feng. Liu[1], H. M. Liu[1], J. Liu[1], J. P. Liu[19], T. R. Liu[1], R. G. Liu[1], Y. Liu[1], Z. X. Liu[1], X. C. Lou[18], G. R. Lu[6], F. Lu[1], J. G. Lu[1], Z. J. Lu[1], X. L. Luo[1], E. C. Ma[1], J. M. Ma[1], R. Malchow[5], H. S. Mao[1], Z. P. Mao[1], X. C. Meng[1], X. H. Mo[1], J. Nie[1], S. L. Olsen[16], D. Paluselli[16], H. Park[9], F. Porter[2], Z. D. Nie[1], N. D. Qi[1], X. R. Qi[1], C. D. Qian[13], J. F. Qiu[1], Y. K. Que[1], G. Rong[1], Y. Y. Shao[1], B. W. Shen[1], D. L. Shen[1], H. Shen[1], X. Y. Shen[1], H. Y. Sheng[1], F. Shi[1], H. Z. Shi[1], X. F. Song[1], H. S. Sun[1], L. F. Sun[1], Y. Z. Sun[1], S. Q. Tang[1], W. Toki[5], G. L. Tong[1], J. Wang[1], J. Z. Wang[1], L. Wang[1], L. S. Wang[1], P. Wang[1], P. L. Wang[1], S. M. Wang[1], Y. Y. Wang[1], Z. Y. Wang[1], C. L. Wei[1], N. Wu[1], D. M. Xi[1], X. M. Xia[1], X. X. Xie[1], G. F. Xu[1], Y. Xu[1], S. T. Xue[1], W. B. Yan[1], W. G. Yan[1], C. M. Yang[1], C. Y. Yang[1], G. A. Yang[1], H. X. Yang[1], X. F. Yang[1], M. H. Ye[9], S. W. Ye[17], Y. X. Ye[17], C. S. Yu[1], C. X. Yu[1], G. W. Yu[1], Y. Yuan[1], B. Y. Zhang[1], C. Zhang[1], C. C. Zhang[1], D. H. Zhang[1], H. L. Zhang[1], H. Y. Zhang[1], J. Zhang[1], J. W. Zhang[1], L. Zhang[1], L. S. Zhang[1], P. Zhang[1], Q. J. Zhang[1], S. Q. Zhang[1], X. Y. Zhang[12], Y. Y. Zhang[1], Z. P. Zhang[17], D. X. Zhao[1], H. W. Zhao[1], Jiawei Zhao[17], J. W. Zhao[1], M. Zhao[1], P. P. Zhao[1], W. R. Zhao[1], Y. B. Zhao[1], Z. G. Zhao[1], J. P. Zheng[1], L. S. Zheng[1], Z. P. Zheng[1], B. Q. Zhou[1], G. M. Zhou[1], L. Zhou[1], K. J. Zhu[1], Q. M. Zhu[1], Y. C. Zhu[1], Y. S. Zhu[1], Z. A. Zhu [1], B. A. Zhuang[1], and B. S. Zou[1].

(BES Collaboration)

[1] *Institute of High Energy Physics, Beijing 100039, People's Republic of China*
[2] *California Institute of Technology, Pasadena, California 91125*
[3] *China Center of Advanced Science and Technology, Beijing 100080, People's Republic of China*
[4] *Chonbuk National University, Chonju 561-756, Korea*
[5] *Colorado State University, Fort Collins, Colorado 80523*
[6] *Henan Normal University, Xinxiang 453002, People's Republic of China*
[7] *Huazhong Normal University, Wuhan 430079, People's Republic of China*
[8] *Hunan University, Changsha 410082, People's Republic of China*
[9] *Korea University, Seoul 136-701, Korea*
[10] *Nankai University, Tianjin 300071, People's Republic of China*
[11] *Peking University, Beijing 100871, People's Republic of China*
[12] *Shandong University, Jinan 250100, People's Republic of China*
[13] *Shanghai Jiaotong University, Shanghai 200030, People's Republic of China*
[14] *Seoul National University, Seoul 151-742, Korea*
[15] *Stanford Linear Accelerator Center, Stanford, California 94309*
[16] *University of Hawaii, Honolulu, Hawaii 96822*
[17] *University of Science and Technology of China, Hefei 230026, People's Republic of China*
[18] *University of Texas at Dallas, Richardson, Texas 75083-0688*
[19] *Wuhan University, Wuhan 430072, People's Republic of China*
[20] *Zhejiang University, Hangzhou 310028, People's Republic of China*

(January 15, 2002)

We report the observation of a narrow enhancement near $2m_p$ in the mass spectrum of $p\overline{p}$ pairs from radiative $J/\psi \to \gamma p\overline{p}$ decays. The results are based on an analysis of a 50 million event sample of J/ψ decays accumulated with the BES detector at the Beijing electron-positron collider. If interpreted as a resonance, the mass and width of the observed enhancement are $M = 1884 \pm 2$ (stat) ± 10 (sys) MeV/c^2 and $\Gamma = 14 \pm 5$ (stat) ± 6 (sys) MeV/c^2, which are inconsistent with any known particle.

There is an accumulation of evidence for anomalous behavior in the proton-antiproton system very near the $M_{p\overline{p}} = 2m_p$ mass threshold. The observed cross section for $e^+e^- \to hadrons$ has a narrow dip-like structure at a center of mass (cm) energy of $\sqrt{s} \simeq 2m_pc^2$ [1]. In addition, the proton's time-like magnetic form-factor, determined from high statistics measurements of the $p\overline{p} \to e^+e^-$ annihilation process, exhibits a very steep fall-off just above the $p\overline{p}$ mass threshold [2]. These data are suggestive of a narrow, S-wave triplet $p\overline{p}$ resonance with $J^{PC} = 1^{--}$ and mass near $M_{p\overline{p}} \simeq 2m_p$, which may be related to a narrow dip structure that is observed just above $2m_p$ in diffractive photoproduction of $3\pi^+3\pi^-$ final states [3]. There is no known vector meson resonance that could be associated with such a state. The proximity in mass to $2m_p$ is suggestive of a nucleon-antinucleon bound state, an idea first proposed by Fermi and Yang in 1949 [4]. On the other hand, some authors have proposed that the steep fall-off of the proton's time-like formfactor is a dynamical effect and not due to a nearby resonance [5]. An investigation of the S-wave singlet $p\overline{p}$ system (*i.e.* with $J^{PC} = 0^{-+}$) may help clarify the situation.

The radiative decay process $J/\psi \to \gamma p\overline{p}$ is well suited for studies of the 0^{-+} $p\overline{p}$ system. Charge-parity conservation insures that the $p\overline{p}$ pairs have $C = +1$ and, for invariant masses near $M_{p\overline{p}} = 2m_p$, the p and $\overline{p}$ are expected to be in a relative S-wave. In this letter we report a study of the low mass $p\overline{p}$ pairs produced via radiative decays in a sample of 50 million J/ψ events accumulated in the Beijing Spectrometer (BES) located at the Beijing Electron-Positron Collider (BEPC) at the Beijing Institute of High Energy Physics.

BES is a large solid-angle magnetic spectrometer that is described in detail in ref. [7]. Charged particle momenta are determined with a resolution of $\sigma_p/p = 1.7\%\sqrt{1+p^2(\mathrm{GeV}^2)}$ in a 40-layer cylindrical drift chamber. Particle identification is accomplished by specific ionization (dE/dx) measurements in the drift chamber and time-of-flight (TOF) measurements in a barrel-like array of 48 scintillation counters. The dE/dx resolution is $\sigma_{dE/dx} = 8.4\%$; the TOF resolution is $\sigma_{TOF} = 160$ ps; both systems independently provide more than 3σ separation of protons from any other charged particle species for the entire momentum range considered in this experiment. Radially outside of the time-of-flight counters is a 12-radiation-length barrel shower counter (BSC) comprised of gas proportional tubes interleaved with lead sheets. The BSC measures the energies and directions of photons with resolutions of $\sigma_E/E \simeq 22\%/\sqrt{E(\mathrm{GeV})}$, $\sigma_\phi = 4.5$ mrad, and $\sigma_\theta = 12$ mrad. The iron flux return of the magnet is instrumented with three double layers of counters that are used to identify muons.

For this analysis we use charged tracks with momentum greater than 80 MeV/c that are well fit to a helix originating near the interaction point. Candidate γ's are associated with energy clusters in the BSC that have less than 80% of their total energy in any one readout layer and do not match the extrapolated position of any charged track. Since antiprotons that stop in the material of the TOF or BSC can produce annihilation products that are reconstructed elsewhere in the detector as γ rays, no restrictions are placed on the total number of neutral clusters in the event. We use charged tracks and γ's that are within the polar angle region $|\cos\theta| < 0.8$. We reject events where both tracks are identified as muons, or produce high energy showers in the BSC that are characteristic of electrons. The dE/dx and TOF information for each track are combined to form a proton identification confidence level, $\mathcal{P}_{pid}$. We require that both tracks in the event have $\mathcal{P}_{pid} > 0.02$. Measurements with a sample of tagged protons and antiprotons from kinematically selected $J/\psi \to \Xi^-\Xi^+$ events, where $\Xi^- \to \Lambda\pi^-$, $\Lambda \to p\pi^-$ (plus the charge conjugate decay chain), indicate that the confidence-level distributions are flat. A study based on a kinematically selected sample of $J/\psi \to K^{*\pm}K^\mp \to K^+K^-\pi^0$ events indicate that charged kaons survive this selection with a probability that is less than 1% per track.

We subject the surviving events to four-constraint kinematic fits to the hypotheses $J/\psi \to \gamma p\overline{p}$ and $J/\psi \to \gamma K^+K^-$. For events with more that one γ, we select the γ that has the highest fit confidence level. For multi-γ events, we also make five-constraint fits to the hypothesis $J/\psi \to \pi^0 p\overline{p}$, $\pi^0 \to \gamma\gamma$, for every combination of two γ rays. We select events that have fit confidence level $CL_{\gamma p\overline{p}} > 0.05$ and reject events that have $CL_{\gamma K^+K^-} > CL_{\gamma p\overline{p}}$ or $CL_{\pi^0 p\overline{p}} > 0.001$.

Figure 1 shows the $p\overline{p}$ invariant mass distribution for surviving events. The distribution has a very distinct peak at near $M_{p\overline{p}} = 2.9$ GeV/c^2 that is consistent in mass, width, and yield with expectations for $J/\psi \to \gamma\eta_C$, $\eta_C \to p\overline{p}$, and a narrow low-mass peak at the $p\overline{p}$ mass threshold that is the subject of this analysis.

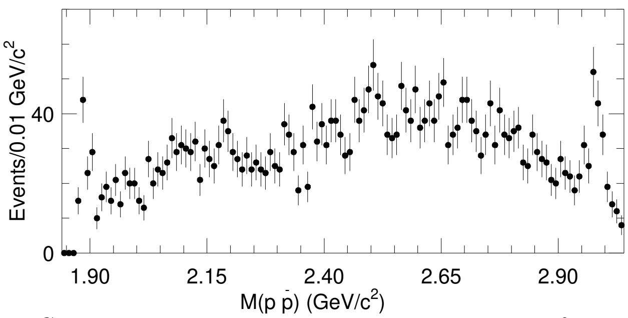

FIG. 1. The $p\overline{p}$ invariant mass distribution for the $J/\psi \to \gamma p\overline{p}$-enriched event sample.

Backgrounds from processes involving charged particles that are not protons and antiprotons are negligibly small. In addition to being well separated from other charged particles by the dE/dx and TOF systems, the protons and antiprotons from the low $M_{p\overline{p}}$ region stop in the TOF counters and, thus, have very characteristic BSC responses: the protons do not produce any matching signals in the BSC while annihilation products from antiproton annihilation can produce large signals. This BSC response is quite distinct from that of K^+K^-, $\pi^+\pi^-$ or e^+e^- pairs, where the positive and negative tracks produce similar, non-zero BSC responses, and is verified with tagged protons and antiprotons from the $J/\psi \to \Xi^-\Xi^+$ sample. The observed BSC energy distributions for the selected $J/\psi \to \gamma p\overline{p}$ events with $M_{p\overline{p}} \leq 1.9$ GeV/c^2 closely match expectations for protons and antiprotons and show no evidence for contamination from other particle species.

There is, however, a large background from $J/\psi \to \pi^0 p\overline{p}$ events, where one of the photons from the $\pi^0 \to \gamma\gamma$ decay is missed. This is studied using a sample of reconstructed $J/\psi \to \pi^0 p\overline{p}$ events that are selected with the same criteria as above except for $CL_{\pi^0 p\overline{p}} > 0.05$, $CL_{\pi^0 p\overline{p}} > CL_{\gamma p\overline{p}}$, and $CL_{\pi^0 p\overline{p}} > CL_{\pi^0 K^+K^-}$. The near-threshold $M_{p\overline{p}}$ distribution for these events, shown in Fig. 2(a), is well fit by a function of the form $f(\delta) = N(\delta^{1/2} + a_1\delta^{3/2} + a_2\delta^{5/2})$, where $\delta = M_{p\overline{p}} - 2m_p$; the fitted function is shown in the figure as a smooth curve. This distribution does not have a narrow peak at low $p\overline{p}$ invariant masses like that seen in the $\gamma p\overline{p}$-enriched sample, shown in Fig. 2(b). Monte Carlo simulations of other J/ψ decay processes with final-state $p\overline{p}$ indicate that background contributions from processes other than $J/\psi \to \pi^0 p\overline{p}$ are negligibly small.

We performed a Monte Carlo study where events are generated as $J/\psi \to \pi^0 p\overline{p}$ with a uniform phase-space distribution and subjected to the same reconstruction and analysis as the data. For events with $M_{p\overline{p}} < 2.15$ GeV$/c^2$, we find $\epsilon_{\pi^0,\gamma}/\epsilon_{\pi^0,\pi^0} = 0.29 \pm 0.01$ where ϵ_{π^0,π^0} is the efficiency for generated $J/\psi \to \pi^0 p\overline{p}$ events to be selected as $\pi^0 p\overline{p}$ by the analysis and $\epsilon_{\pi^0,\gamma}$ is the efficiency that they pass the $\gamma p\overline{p}$ selection.

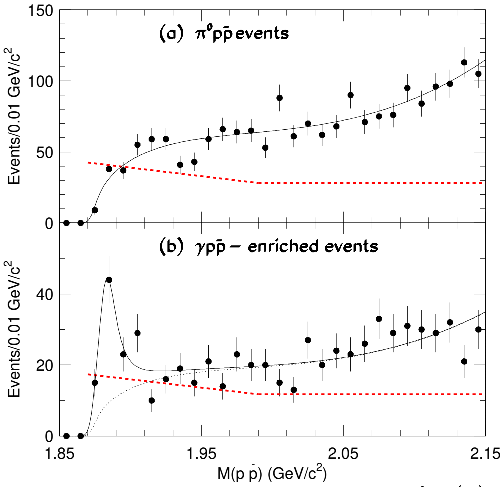

FIG. 2. The $p\overline{p}$ invariant mass distribution for **(a)** selected $J/\psi \to \pi^0 p\overline{p}$ decays and **(b)** the $J/\psi \to \gamma p\overline{p}$-enhanced event sample. The smooth curves are the result of fits described in the text and the dashed curves indicate the mass dependence of the experimental acceptance. The dotted curve in (b) indicates the background component of the fitted curve.

In BES, the detection efficiency for protons and antiprotons falls sharply for three-momenta below 0.4 GeV$/c$. This produces a mass dependence in the experimental acceptance near $M_{p\overline{p}} \simeq 2m_p$ for $J/\psi \to \gamma p\overline{p}$ and $\pi^0 p\overline{p}$. For both processes, when $M_{p\overline{p}}$ is very near $2m_p$, the p and $\overline{p}$ both have three-momenta very near 0.5 GeV$/c$ and are well detected. For increasing $p\overline{p}$ masses, more asymmetric energy sharing is possible and the acceptance decreases until $M_{p\overline{p}} \simeq 2.0$ GeV$/c^2$, where it is $\simeq 0.67$ of its value at $M_{p\overline{p}} = 2m_p$. Although this acceptance variation, shown as dashed lines in Figs. 2(a) and (b), enhances the near-threshold mass distributions, it is evident that it neither produces a low-mass peak in the $J/\psi \to \pi^0 p\overline{p}$ background (Fig. 2(a)) nor can account for the narrow peak that is observed in the $\gamma p\overline{p}$-enriched spectrum (Fig. 2(b)).

The smooth curve in Fig. 2(b) is the result of a fit using a background with the functional form of $f(\delta)$ used to fit the $\pi^0 p\overline{p}$ data of Fig. 2(a), with shape parameters a_1 and a_2 fixed at the values determined from that fit, plus an acceptance-weighted, S-wave Breit-Wigner (BW) function with mass and width that are allowed to vary. In all fits the fitting functions are convolved with a Gaussian resolution function with $\sigma = 3$ MeV, its Monte-Carlo determined value. This fit yields a total of 75.0 ± 13.8 events in the BW function with a mass $M = 1884 \pm 2$ MeV$/c^2$ and a full width $\Gamma = 14 \pm 5$ MeV. For this fit, $\chi^2/d.o.f. = 24.1/24$, and the normalization of the background function, which is 0.30 ± 0.03 times that for the $\pi^0 p\overline{p}$ fit, agrees well with the MC value for $\epsilon_{\pi^0,\gamma}/\epsilon_{\pi^0,\pi^0}$. This indicates that the background is consistent with being almost entirely due to feed-down from $J/\psi \to \pi^0 p\overline{p}$ decays, although a small fraction of non-resonant $\gamma p\overline{p}$ cannot be excluded.

We determine the significance of the observed peak from $\Sigma = \sqrt{-2\ln(\mathcal{L}_0/\mathcal{L}_{\max})}$, where $\mathcal{L}_{\max}$ is the likelihood for the nominal signal yield and $\mathcal{L}_0$ is the value for a fit with background only. Figure 3(a) shows the result of a fit using f_{bkg} alone, with the normalization (N) allowed to float and shape parameters fixed from the fit to the $\pi^0 p\overline{p}$ sample. The fit results give $\Sigma = 9.4\sigma$.

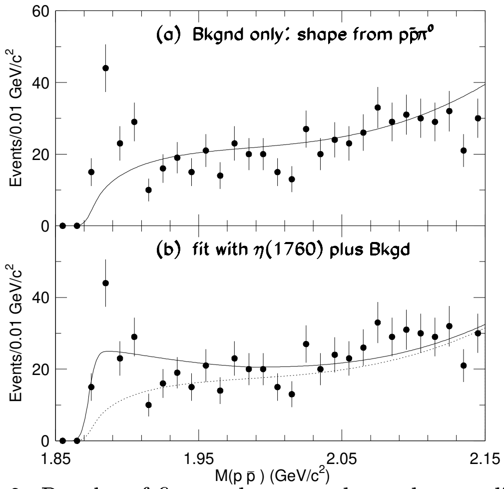

FIG. 3. Results of fits to the $\gamma p\overline{p}$-enhanced mass distribution with **(a)** background only with a shape determined from the fit to the $\pi^0 p\overline{p}$ sample and **(b)** an S-wave BW function with mass and width of the $\eta(1760)$ plus a background (dotted curve) with the $\pi^0 p\overline{p}$ shape.

We tried to fit the data using known particle resonances to represent the low-mass peak. Since the peak is very close to threshold, we restrict ourselves to the case where the p and $\overline{p}$ are in an S-wave, which implies a $J^{PC} = 0^{-+}$ pseudoscalar state. There are two pseudoscalar resonances listed in the PDG tables in this mass region [6]: the $\eta(1760)$ with $M_{\eta(1760)} =$

1760 ± 11 MeV/c^2 and $\Gamma_{\eta(1760)} = 60 \pm 16$ MeV, and the $\pi(1800)$ with $M_{\pi(1800)} = 1801 \pm 13$ MeV/c^2 and $\Gamma_{\pi(1800)} = 210 \pm 15$ MeV. Figure 3(b) shows the result of a fit with f_{bkg} with shape parameters fixed from the $\pi^0 p\bar{p}$ fit and an acceptance-weighted S-wave BW function with mass and width fixed at the PDG values for the $\eta(1760)$. This fit has a $\chi^2/d.o.f. = 49.1/26$, which corresponds to a fit confidence level of $CL = 0.4\%$. A fit with the $\pi(1800)$ parameters gives a slightly worse fit ($CL = 0.15\%$).

Although the fit that includes the $\eta(1760)$ gives a marginally acceptable fit for the whole mass range it is evident from Fig. 3(b) that the main contributions to the χ^2 value comes from the low-mass region, where the fitted function does not represent the data very well. To compare the relative significance of the fit with the narrow BW signal to that with the $\eta(1760)$, we repeated the fit with f_{bkg} and the $\eta(1760)$ *plus* an S-wave BW component with mass and width allowed to vary. With this addition, the fitted value of the $\eta(1760)$ normalization goes to zero and the parameters of the added BW and the f_{bkg} normalization are identical to those from the fit shown above in Fig. 2(b). From a comparison of the $\ln \mathcal{L}$ values for the fits that include an $\eta(1760)$ with and without the narrow BW term, we find the narrow state is favored by $\Sigma = 4.5\sigma$.

We verified that the observed low-mass signal originates from J/ψ decays and does not come from a radiative-return process $e^+e^- \rightarrow \gamma p\bar{p}$, where the γ is due to initial-state radiation, by searching for a similar signal in a sample of 3.8 million $\psi(2S)$ decays, also accumulated in the BES detector. If the observed peak is associated with J/ψ decays, we expect $n_{\psi(2S)}$, the number of events in the $\psi(2S)$ sample, to be of order $n_{\psi(2S)} \simeq 0.01 n_{J/\psi} \sim 1$ event, where $n_{J/\psi}$ is the number of events in the low-mass peak in the J/ψ data [8]. In contrast, if the observed peak is due to radiative return, we expect $n_{\psi(2S)} \simeq 0.20 n_{J/\psi} \sim 15$ events [9]. An application of the selection criteria to the $\psi(2S)$ event sample results in only one surviving event with $M_{p\bar{p}} < 1.9$ GeV; this strongly rules out the radiative-return hypothesis.

For a pseudoscalar $p\bar{p}$ state, the polar angle of the photon, θ_γ, is expected to have a $1+\cos^2\theta_\gamma$ distribution. Figure 4 shows the acceptance-corrected $|\cos\theta_\gamma|$ distribution for events with $M_{p\bar{p}} \leq 1.90$ GeV and $|\cos\theta_\gamma| \leq 0.8$. The solid curve shows the result of a fit for $1+\cos^2\theta_\gamma$ to the $|\cos\theta_\gamma| < 0.8$ region. The data are in agreement with expectations for pseudoscalar production.

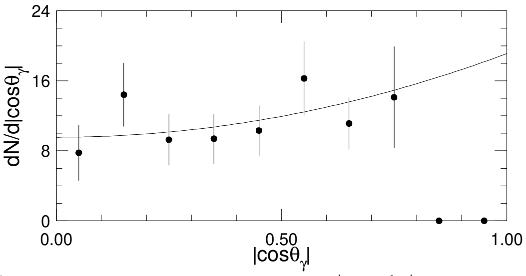

FIG. 4. The acceptance-corrected $|\cos\theta_\gamma|$ distribution for $J/\psi \rightarrow \gamma p\bar{p}$-enriched events with $M_{p\bar{p}} \leq 1.9$ GeV/c^2. The curve is a fit to a $1+\cos^2\theta_\gamma$ shape for the region $|\cos\theta_\gamma| \leq 0.8$.

If a resonance mass value is below threshold, the observed peak position is not strongly related to the actual mass value. In Monte Carlo simulations we find that an observed mass value of 1884 MeV/c^2 can be produced by a resonance at that mass *or* by a subthreshold state with mass just below the $p\bar{p}$ threshold of 1876 MeV/c^2. We include this difference in the systematic error on the mass. Other systematic errors on the mass and width are determined by redoing the fits with: MC-generated background shapes; background shape parameters that are free to vary; inflated and deflated resolutions; and increased and decreased mass-dependent acceptance variations. We include the extreme variations in the results into the systematic error. We find $M = 1884 \pm 2 \pm 8$ MeV/c^2 and $\Gamma = 14 \pm 5 \pm 6$ MeV/c^2; the first errors are statistical and the second systematic.

Using a Monte-Carlo determined acceptance of 0.29 ± 0.03, we determine a product of branching fractions $\mathcal{B}(J/\psi \rightarrow \gamma X(1875))\mathcal{B}(X(1875) \rightarrow p\bar{p}) = (5.2 \pm 1.0^{+1.8}_{-0.7}) \times 10^{-6}$, where the systematic error includes uncertainties in the acceptance, the total number of J/ψ decays in the data sample (5%), and the effects of changing the various inputs to the fit (+23% -4%).

The structure that we see is not the obvious effect of any known meson resonance. If interpreted as a resonance, its peak mass and total width are near the corresponding values found for the hypothesized vector nucleon-antinucleon state (1870 ± 10 MeV/c^2 and 10 ± 5 MeV, respectively) that is used in ref. [1] to reproduce the dip structure that is observed in the $e^+e^- \rightarrow$ *hadron* annihilation cross section.

We acknowledge the strong efforts of the BEPC staff and the helpful assistance we received from the members of the IHEP computing center. This work is supported in part by the National Natural Science Foundation of China under Contract Nos. 19290400, 19991480, 19805009 and 19825116; the Chinese Academy of Sciences under contract Nos. H-10, KG95P-03, and E-01 (IHEP); and by the Department of Energy under Contract Nos. DE-FG03-93ER40788 (Colorado State University), DE-AC03-76SF00515 (SLAC), DE-FG03-94ER40833 (U Hawaii), DE-FG03-95ER40925 (UT Dallas), and by the Ministry of Science and Technology of Korea under Contract KISTEP I-03-037(Korea).

[1] A. Antonelli *et al.* , Nucl. Phys. **B517**, 3 (1998).
[2] G. Bardin *et al.* , Nucl. Phys. **B411**, 3 (1994).
[3] P.L. Frabetti *et al.* (E687 collaboration), Phys. Lett. **B514**, 240 (2001).
[4] E. Fermi and C.N. Yang, Phys. Rev. **76**, 1739 (1949). For a recent review of this subject, see J-M. Richard, Nucl. Phys. Proc. Suppl. **86**, 361 (2000).
[5] See, for example, M. Karliner, hep-ph/0112047.
[6] D. Groom *et al.* (Particle Data Group), Eur. Phys. Jour. **C15**, 1 (2000).
[7] J.Z. Bai *et al.* (BES Collaboration), Nucl. Instr. Meth. **A344**, 319 (1994).
[8] If the signal is from J/ψ decays, the expected event yield in the $\psi(2S)$ data sample is

$$n_{\psi(2S)} \sim n_{J/\psi} \times \frac{N_{\psi(2S)}}{N_{J/\psi}} \times 0.14 \simeq\ 0.01 \times n_{J/\psi},$$

where $N_{J/\psi}$ and $N_{\psi(2S)}$ are the total number of J/ψ and $\psi(2S)$ events, and the factor of 0.14 takes into account the charmonium cascade decay channels of the $\psi(2S)$ that are not accessible the the J/ψ, as first proposed by T. Applequist and D. Politzer, Phys. Rev. Lett. **34**, 43 (1975).
[9] If the signal is due to radiative return, an application of the formalism of G. Bonneau and F. Martin, Nucl. Phys. **B27**, 381 (1971) gives an expected event yield in the $\psi(2S)$ data sample of

$$n_{\psi(2S)} = n_{J/\psi} \times \frac{\mathcal{L}(\psi(2S))}{\mathcal{L}(J/\psi)} \frac{f(k_{\psi(2S)})}{f(k_{J/\psi})} \frac{M^2_{J/\psi}}{M^2_{\psi(2S)}} = 0.20 \times n_{J/\psi},$$

where $\mathcal{L}(J/\psi)$ and $\mathcal{L}(\psi(2S))$ are the luminosities (17.7 and 6.0 pb^{-1} for the J/ψ and $\psi(2S)$, respectively) and $f(k)$ is a function that describes the effective luminosity as a function of $k = 1 - 4m_p^2/s$, the fractional cm energy of the initial-state-radiation photon.